

Simulation and Experimental Study of Terahertz Band-Stop Filter Based on Parallel Corrugated Metal Plates

Liu Xiang, Yang Dongxiao, Yu Chunyan
 a) College of Information Science & Electronic Engineering
 Zhejiang University
 Hangzhou 310027, China
 b) Research Center for Terahertz Technology
 Zhejiang University
 Hangzhou 310027, China

Abstract — A terahertz band-stop filter was proposed based on the transmission properties of parallel metal plates with corrugated grating grooves. The influence of distance w between two corrugated plates and mismatch length l of two plates were simulated and experimentally studied. The bandwidth of the stop-band increases with the decreasing of w . The filter can be optimized by adjusting l . The optimal filter can be achieved by adjusting l to half the period of grating grooves.

Key words - Terahertz; Surface plasmon; Bandgap; Metal grating;

I. INTRODUCTION

The study of surface plasmon polaritons (SPPs) in terahertz (THz) frequency region has significant scientific and technological potentials. [1-3] In THz frequency region, however, the metal's properties approach to those of perfect electrical conductor (PEC) which induced the SPPs localized very weakly on surface. [4] Groove grating corrugated on the metal surface is a structure for guiding THz SPPs on metal surface. The periodic structure could provide momentum compensation to incident THz wave and arouse SPPs resonance. Since Pendry *et al.* [5] examined SPPs on corrugated metal surface, lots of significant researches have been reported recent years. [6-7]

In this work, a band-stop filter was proposed based on the THz transmission properties of parallel corrugated metal plates (PCMP). The transmission properties were simulated and experimentally demonstrated.

II. SIMULATIONS AND DISCUSSION

It has been generally accepted that the highly confined propagation mode can be achieved by corrugating periodic structures on metal surface. The periodic structure provides a wave-vector compensation for SPPs to satisfy phase matching condition. This relation is that the wave-vector k_x of the incident terahertz radiation, plus the corrugated structure wave-vector compensation with a magnitude $2\pi/d$ equals the scattered SPPs wave-vector. Using modal expansion method, the first-order approximation dispersion relation of spoof SPPs can be represented as:[8]

$$\frac{\sqrt{k_x^2 - k_0^2}}{k_0} = \frac{a}{d} \tan(k_0 h) \tag{1}$$

Since the wave-vector in free space is $k_0 = \omega/c$ (c is the light speed in vacuum), the SPP wave-vector along the propagation direction of incident wave can be obtained from the dispersion relation and rewritten as:

$$k_x = \frac{\omega}{c} \sqrt{\frac{a^2}{d^2} \tan^2\left(\frac{\omega}{c} h\right) + 1} \tag{2}$$

Equation (2) indicates that the wave-vector of SPPs on corrugated metal plate surface varies with the geometry parameters of the surface structure.

Figure. 1 shows the schematic configuration of the PCMP structure and its corresponding geometry parameters. The period of the grating grooves was labelled as d ; w was the distance between the plates; a and h were the width and depth of grooves, respectively; l was the mismatch length between two plates.

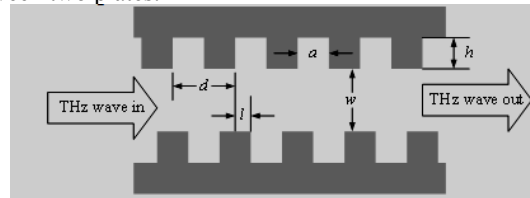


Figure. 1 Schematic structure of the PCMP and its corresponding geometry parameters.

In this work, the geometry parameters of groove gratings were $a = 160 \mu\text{m}$, $d = 2*a = 320 \mu\text{m}$, $h = 120 \mu\text{m}$ in both simulations and experiments. Using the equations above, we can calculate that the SPP resonance frequency of the plates compose the PCMP structure is about 0.33 THz.

Simulations were implemented to obtain the dispersion relations and transmission spectra of the PCMP structure by using COMSOL Multiphysics software, which was based on the Finite Elements Methods (FEM).

In simulations, the metal material was set as Perfect Electric Conductor (PEC), material between two plates was set as air. The input terahertz was set as TM mode since only TM wave can excite SPPs. [9]

Figure. 2 show the simulation results with $w = d = 320 \mu\text{m}$, $l = 0$. The frequency and wave-vector are normalized by

the period d . The transmission spectrum is rotated 90 degree anticlockwise to better understand the corresponding relations. According to the dispersion curve in Fig. 2, there existed two bandgaps which are marked as Bandgap 1 and Bandgap 2, respectively. Two gaps are well corresponding to stop-bands in the transmission spectrum. The dispersion curve corresponding to passband in lower frequency range ($d/\lambda \leq 0.32$) is below light cone which means it is surface plasmon (SP) mode. In addition, the SP mode curve of PCMP structure is further away from light cone than that of single corrugated metal plate,[8] it means that the SP wave is better confined on the surface of PCMP structure.[9] Electromagnetic wave confined on two plates are coupled each other and propagate along PCMP instead of scattering to free space as single layer. The start frequency of Stopband 1 equals 0.3 THz ($d/\lambda = 0.32$) and approaches to the resonance frequency of corrugated metal plate, which also indicates that the propagating wave at lower frequency is SPP mode.

The other dispersion curves above the light cone are waveguide mode. Bandgap 1 is between the pass-bands of SP mode and waveguide mode. Bandgap 2 is only dominated by waveguide mode. The band-stop filter is designed utilizing the properties of Bandgap 1 in this work.

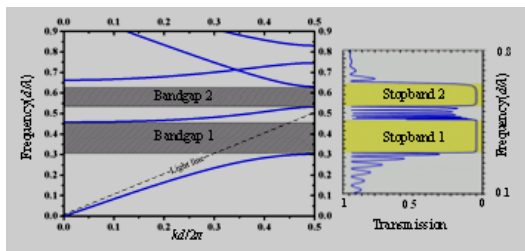
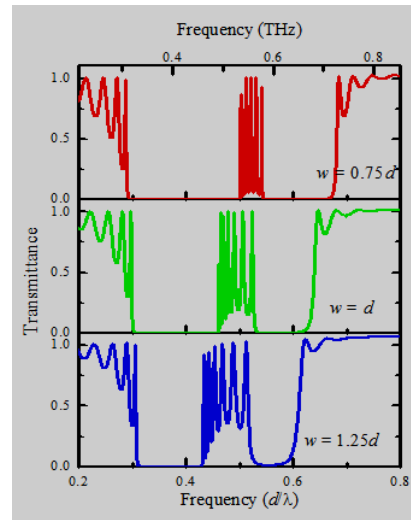
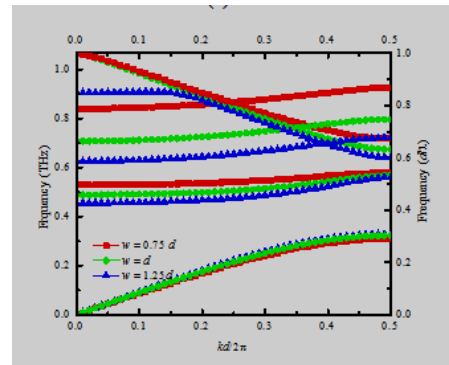


Figure. 2 Dispersion relations of PCMP ($l = 0$ mm, $w = 320$ μ m) and its transmission spectrum.

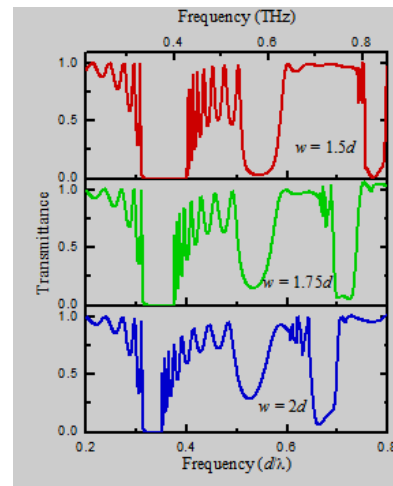
Furthermore, the transmission spectra of PCMP with different distance w and l were simulated and compared. Figure. 3 shows the transmission spectra of PCMP with several w values between 240 μ m ($0.75*d$) and 640 μ m ($2*d$) and their corresponding dispersion curves. It is evident from Figure. 3 that the width of Stopband 1 decreased with the increasing of w . Since the SPP resonance frequency is decided by the geometry parameters of the corrugated structure, the lower cut-off frequency of Stopband 1 remains almost unchanged with different parameters w especially when w is larger than $1.5d$. The waveguide mode was mainly effected by w , which causes the cut-off frequency of Stopband 1 varies as the changing of w . When $w = 2d$, the Stopband 2 disappeared, as shown in Figure. 3. Thus the bandwidth of Stopband 1 is decided by w of PCMP while the lower cut-off frequency of Stopband 1 is decided by the geometry parameters of corrugated metal.



(a)

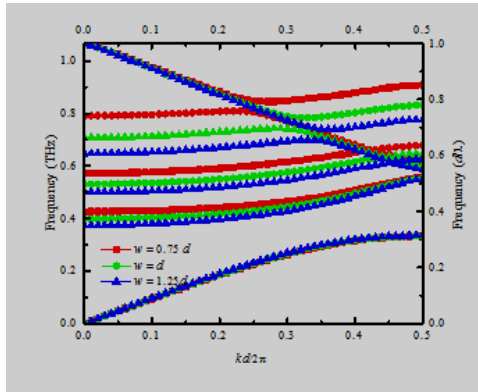


(b)



(c)

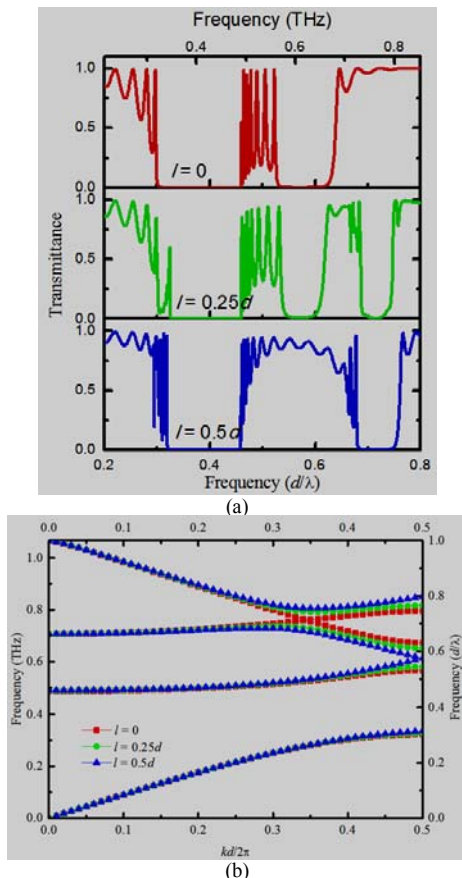
Continued on next page.



(d)

Figure 3 Transmission spectra of the PCMP ($a = h = d/2 = 160 \mu\text{m}$, $l = 0$) with different distance between two corrugated plates w compared with its corresponding dispersion curves.

The transmission spectra of PCMP with some l values and their corresponding dispersion curves are plotted in Figure 4. According to Fig. 4, the variation of mismatch l have almost no effect on Stopband 1, but have great influence on Stopband 2. Stopband 2 diminishes with the increasing of l . Specifically, Stopband 2 disappeared with mismatch $l = d/2$ which makes the optimal band-stop filter.



(a)

(b)

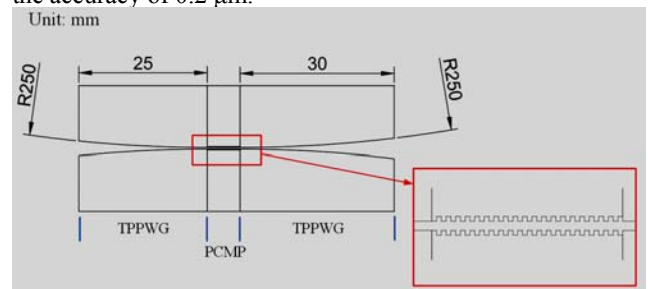
Figure 4 Transmission spectra of the PCMP ($a = h = d/2 = 160 \mu\text{m}$, $w = 320 \mu\text{m}$) with different l compared with the corresponding dispersion curves.

III. EXPERIMENTAL SECTION

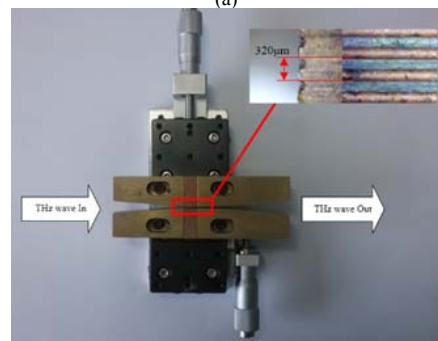
According to the simulated results discussed in section 2, the PCMP structure was fabricated for experiments. Because the beam diameter of incident THz wave is much larger than the plates' separation, couplers are needed to enhance the incident energy.

The experimental devices are shown in Fig. 5. Figure 5(a) shows the schematic structure of the experimental sample. Two couplers made of round-type tapered parallel-plate waveguides (TPPWG) are set on both sides of PCMP, which can enhance the coupling efficiency obviously. [10] The couplers are set with length of 2.5 cm on entrance port and 3 cm on exit port (The lengths were limited by the size of the sample chamber in experiments) and were both with a 250mm-diameter circular arc. The metal material of PCMP and TPPWG structure we choose is copper which can be considered as a PEC in the THz region

The fabricated sample is shown in Figure. 5(b), the inset in the top-right is the partial enlarged detail of grating grooves photographed with microscope. The parameters of sample are consistent with that in simulations: the grating period is $320 \mu\text{m}$ and the width and depth of grooves are $160 \mu\text{m}$ and $120 \mu\text{m}$. All devices are fixed on two precision stage position tables which can provide precise variation of w with the accuracy of $0.2 \mu\text{m}$.



(a)



(b)

Figure 5 (a) The schematic structure of the experimental device: PCMP structure with TPPWG structure couplers on both sides. (b) The fabricated sample fixed on two displacement plate.

Inset: optical microscope image of several unit cells with scale.

In this work, the transmission spectra of the sample was measured by terahertz time domain spectroscopy (THz-TDS) system with available spectrum range from 0.1 to 2.0 THz and resolution of 5 GHz. The ambient temperature was

around 27°C. In order to get the transmitting properties effectively, the reference signal was obtained by measuring the waveform of the transmitted THz waves through TPPWG couplers without PCMP structure, a brass layer with 3 mm diameter aperture was set in front of the incident side of experimental device to prevent the incident wave direct to the detector.

Transmission spectrum of the sample with $w = 320\mu\text{m}$ and mismatch length $l = 0$ is showed in Fig.6 comparing with its corresponding simulated result. Two spectra show the same tendency.

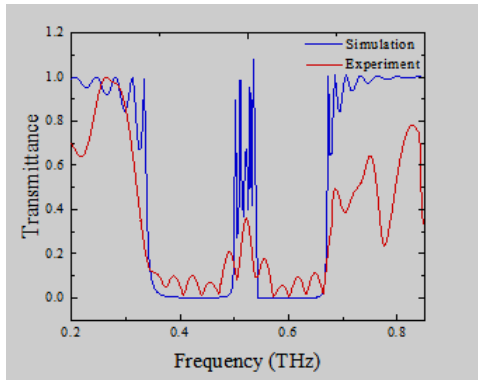


Figure. 6 Measured and simulated transmission spectra of PCMP with $w = 0.32\text{ mm}$, $l = 0$.

Figure. 6 shows that the variation tendency of the experiment result is in agreement with the simulation result. Some subtle differences was caused by some unavoidable factors. The fabricate accuracy, surface smoothness of the material would induce some difference of measured results. The water vapor in testing system would influence the experimental results as well.

Then the transmission spectra were measured by adjusting the distance between two plates without

mismatching. Fig.7 shows the transmission spectra of PCMP with $w = 0.32\text{ mm}$, 0.48 mm and 0.64 mm . It can be observed that the change tendency of the stop-band (Stopband 1) width and its upper and lower cut-off frequency are in accordance with the simulation results above.

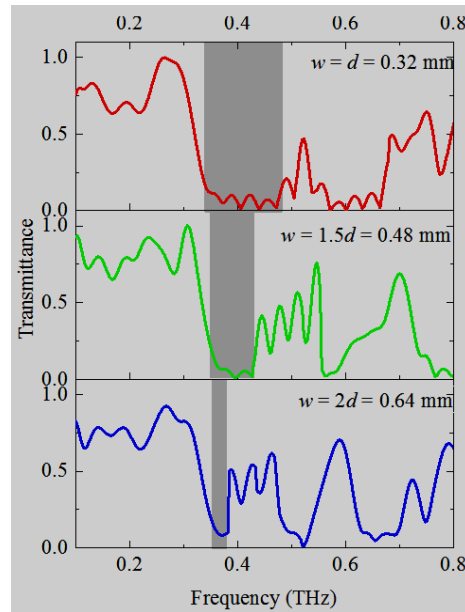


Figure. 7 Transmission spectra of PCMP with $l = 0$ and different d ($d = 0.64\text{ mm}$, $d = 0.48\text{ mm}$, $d = 0.32\text{ mm}$).

In order to better clarify the influence of w on the Stopband 1, Table 1 lists the lower, upper cut-off frequency and bandwidths of the stop-band at several w values.

TABLE I LOWER, UPPER CUT-OFF FREQUENCY, AND 3-DB BANDWIDTHS OF STOPBAND 1 AT SEVERAL w VALUES.

w (mm)	measured results			simulation results		
	lower cut-off frequency (THz)	upper cut-off frequency (THz)	bandwidth (THz)	lower cut- off frequency (THz)	upper cut-off frequency (THz)	bandwidth (THz)
0.24	0.320	0.521	0.201	0.305	0.518	0.213
0.32	0.322	0.499	0.177	0.310	0.491	0.181
0.40	0.325	0.445	0.120	0.314	0.447	0.129
0.48	0.340	0.430	0.090	0.330	0.416	0.086
0.56	0.347	0.409	0.058	0.331	0.400	0.069
0.64	0.350	0.394	0.044	0.333	0.382	0.049

The measured results indicate that the lower cut-off frequency of Stopband 1 remained almost stationary when $w \geq 1.5d$ and is near the resonance frequency of SPPs. When w is smaller than $1.5d$, the electromagnetic wave confined on two plates make larger effect of each other, which makes the dispersion curve further away from light cone, thus lower cut-off frequencies become lower. But it also is a small variation. This proved that the lower cut-off frequency is decided by the grating period. The Varying w value can change the start frequency of waveguide mode, which

changes the upper cut-off frequency of the stop-band. The measured results accord closely with the simulations.

As a band-stop filter, property showed in Fig. 8 is not very satisfactory. Mismatch l is used for property optimization. According to the simulation results showed before, $l = 0.5d$ was chosen in experiments. Transmission spectra showed in Figure. 8 are the comparison of the PCMP structure with $l = 0.5d$ and $l = 0$. It was apparent that mismatch made PCMP a better property as a band-stop filter

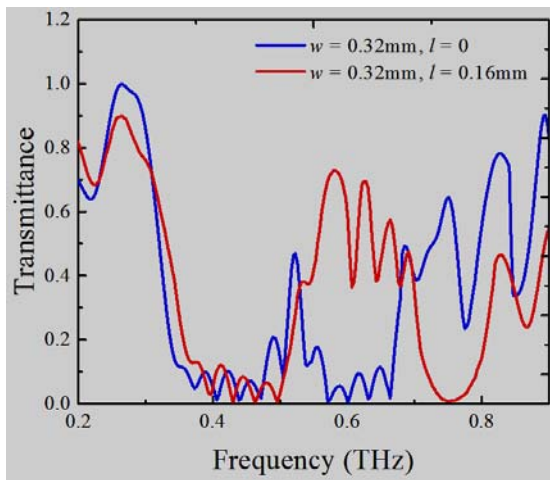


Figure. 8 Comparison of measured transmission spectra of PCMP with $w = 0.32 \text{ mm}$, $l = 0$ and $w = 0.32 \text{ mm}$, $l = d/2 = 0.16 \text{ mm}$

In order to study the effect of parameter w on the optimized PCMP structure with mismatch, we adjusted w of the PCMP structure with mismatching length $l = d/2 = 0.16 \text{ mm}$ and measured the transmission spectra showed in Fig. 9.

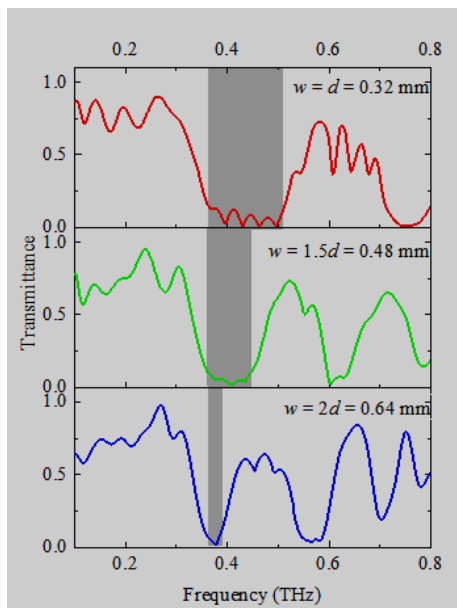


Figure. 9 Transmission spectrum of PCMP with $l = d/2 = 0.16 \text{ mm}$ and different d ($d = 0.64 \text{ mm}$, $d = 0.48 \text{ mm}$, $d = 0.32 \text{ mm}$).

It is evident from the spectra that when distance w become larger, the width of the stop-band become narrower, but the lower cut-off frequency of the stop-band almost kept unchanged. Parameter w could be used to control the stop-band width of the optimized structure.

Furthermore, parameter h (depth of grooves), parameter a/d (the ratio of groove width and groove period) could adjust the stop-band width and the lower cut-off frequency. Because of the processing difficulties, the adjustment using these parameters was uneconomic. Consequently, we mainly focused on the influence of w and l in this work.

IV. CONCLUSIONS

To summarize, the transmission characteristics of PCMP structure are demonstrated in this work which exhibited band-stop properties. Since the SPP mode propagated at lower frequency and the waveguide mode at higher frequency, the lower cut-off frequency of the bandgap is decided by geometry parameters of corrugated plates while the higher cut-off frequency is decided by the distance between two parallel plates. Both simulations and experiments certified that conclusion. The bandwidth of stop-band can be adjusted by varying distances between two plates. The optimal filter was achieved by applying mismatch l of two plate to half of grating's period. In a sense, the properties of the PCMP structure lay foundations for potential band-stop filters.

REFERENCES

- [1] Federici J and Moeller L 2010 J. Appl. Phys. 107 111101.
- [2] Zhang J Q and Grischkowsky D 2004 Opt. Lett. 29 1617
- [3] Zhong R B, Liu W H, Zhou J and Liu S G 2012 Chin. Phys. B 2012 21 117303
- [4] Dragoman M and Dragoman D 2008 Prog. Quant. Electron. 32 1
- [5] Pendry J B, Holden A J, Stewart W J and Youngs I 1996 Phys. Rev. Lett. 76 4773
- [6] Chen L, Cheng Z X, Xu J M, Zang X F, Cai B and Zhu Y M 2014 Opt. Lett. 39 4541
- [7] Xia S, Yang D X, Li T, Liu X and Wang J 2014 Opt. Lett. 39 1270
- [8] Williams C R, Andrews S R, Maier S A, Fernández-Domínguez A I, Martín-Moreno L and García-Vidal F J 2008 Nature Photonics 2 175
- [9] Barnes W L, Dereux A and Ebbesen T W 2003 Nature 424 824
- [10] Kim S H, Lee E S, Ji Y B and Jeon T I 2010 Opt. express 18 1289